

Application of laser induced breakdown spectroscopy for determination of sodium in ice

Morimasa TAKATA^{1*}, Kumiko GOTO-AZUMA^{2*}, Yoshiro ITO¹, Nobuhiko AZUMA¹ and Hisako KANDA^{2**}

¹ Nagaoka University of Technology, Nagaoka, Niigata 940-2188 Japan

² Nagaoka Institute of Snow and Ice Studies, Nagaoka, Niigata 940-0821 Japan

(Received October 23, 2001 ; Revised manuscript received November 21, 2001)

Abstract

We have developed a continuous and non-destructive technique to analyze chemical constituents in ice that uses laser-induced breakdown spectroscopy (LIBS). In an earlier paper, we showed that this method can determine the calcium concentrations in ice. In this paper, we apply the same technique to determine sodium concentrations in ice. First, we quenched sprayed thin layers of standard sodium solutions in succession to build up thick ice samples containing known concentrations of Na. Then, the emission of Na around a wavelength of 589 nm was measured when the ice samples were irradiated with focused laser pulses. The volume of ice consumed for each measurement was only about 1 mm in both diameter and depth. Under nearly optimal conditions, the emission intensity was proportional to sodium concentration when the latter were 10 – 200 $\mu\text{g g}^{-1}$. We also found a linear relationship in the high concentration range (10 – 1000 $\mu\text{g g}^{-1}$). The detection limit was estimated to be 17 $\mu\text{g g}^{-1}$. These results indicate that LIBS can be used to analyze sodium in sea ice, although a much lower detection limit is needed to analyze ice cores.

1. Introduction

Variations of chemical species in ice cores and sea ice provide information on the history of environmental changes and sea ice growth, respectively (e.g. Oesheger and Langway, 1989; Weeks and Ackly, 1982). Conventional chemical analysis techniques, such as ion chromatography, atomic absorption spectroscopy, and inductively-coupled plasma mass spectrometry (ICP-MS), require liquid samples. These techniques usually require cutting the ice samples, removing the sample surface for decontamination, and melting the decontaminated samples in cleaned bottles. This sample preparation procedure is very time-consuming, which limits the number of samples measured; hence, this method makes it difficult to analyze chemical species with high spatial resolution. To solve this problem, Sigg *et al.* (1994) developed a method called continuous flow analysis (CFA) that can determine H_2O_2 , HCHO, NH_4^+ , and Ca^{2+} at a sampling resolution of 1 – 3 cm without cutting the ice samples. Improved CFA can determinate eight chemical components with approximately 1 cm resolution (Röthlisberger *et al.*, 2000). The CFA, however, uses large sample volumes and cannot determine the chemical

constituents in thin characteristic layers, such as cloudy bands (e.g. Meese *et al.*, 1997), because the uncertainty of measurement location in the sample is approximately ± 1 cm. The purpose of our research is to develop a chemical analysis technique that can determine various chemical species in ice samples with spatial resolution and positioning accuracy of 1 – 2 mm.

To determine chemical elements in solid ice samples at mm-resolution without melting the samples, we have made the first application of laser induced breakdown spectroscopy (LIBS) to ice. (For previous work with LIBS, see Radziemski and Cremers, 1989; Kagawa and Yokoi, 1982; Cremers and Radziemski, 1983; Radziemski *et al.*, 1983; Cremers *et al.*, 1984; Kitamori *et al.*, 1989; Iida, 1990; Kagawa *et al.*, 1995; Ito *et al.*, 1995; Nakamura *et al.*, 1996.) Before we apply this technique to real ice core and sea ice samples, the following procedure is necessary (Takata *et al.*, 2000): (1) prepare homogeneous, standard ice samples containing known concentrations of a chemical species, (2) detect the characteristic emission spectrum corresponding to the chemical species from laser-induced breakdown plasma, (3) find the optimal conditions of laser irradiation and spectral measure-

*Present address: National Institute of Polar Research, 1-9-10 Kaga, Itabashi-ku, Tokyo 173-8515 Japan

**Present address: Nagaoka University of Technology, Nagaoka, Niigata 940-2188 Japan

ments, (4) determine the relationship between emission intensity and concentration of chemical species in standard ice samples, and (5) apply the method to various chemical species. So far we have carried out steps (1) – (4) with artificial ice samples containing either calcium (Ca) or sodium (Na). Previously, we reported on steps (2) – (4), using the results for Ca (Takata *et al.*, 2000). Here we report the results of steps (1) – (4) for Na.

2. Preparation of standard ice samples

Artificial ice samples containing known, homogeneous concentrations of Na are required to investigate the relation between the Na concentration and the emission intensity from Na. Standard ice sample preparation techniques for x-ray analysis have been reported (Wyness *et al.*, 1987; Reid *et al.*, 1992). However they were thin (thickness less than 1 mm) and high concentration ($10^2 - 10^4 \mu\text{g g}^{-1}$) samples. In this study, we developed the following sample preparation method to make samples that are thicker and have lower concentrations than those of Wyness *et al.* (1987) and Reid *et al.* (1992): (i) A $1000 \mu\text{g g}^{-1}$ solution of Na was prepared from reagent grade, 99.9% pure, NaCl and ultra pure water of 18 M Ω resistance. (ii) Solutions at lower concentrations were prepared by diluting the $1000 \mu\text{g g}^{-1}$ solution. (iii) A solution of designated concentration was cooled to about 0 °C. (iv) Copper plates of dimension $20 \times 20 \times 2$ mm were first cleaned with acetone and ultra pure water of 18 M Ω resistance and then cooled to -20 or -50 °C. (v) The cooled solution was sprayed on the cooled copper plates using an atomizer to form a thin layer of ice, less than 1 mm thick. The sprayed solution froze immediately upon contact and formed a thin layer (see Fig. 1). (vi) The copper plates with the thin ice layers were cooled again to -20 or -50 °C. (vii) Steps (v) and (vi) were repeated more than 10 times so that the final

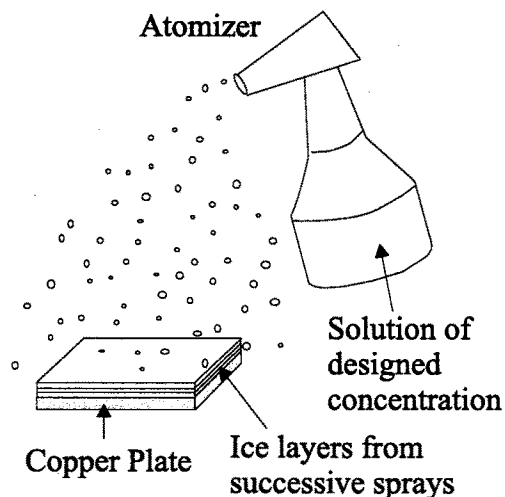


Fig. 1. Method of sample preparation.

ice thickness was about 10 mm. The sample density was about $0.88 \times 10^3 \text{ kg m}^{-3}$, and crossed-polaroids measurements on thin sections showed that the grain size of the samples was about 0.5 mm.

3. Equipment

Figure 2 provides a schematic representation of the experimental set-up, which is basically the same as that described by Takata *et al.* (2000). An ice sample to be analyzed was mounted in a chamber that was kept at about -5 °C. We used a Q-Switched Nd:YAG laser (Spectrum Physic model DCR-3G) of 8 ns pulse width that had a wavelength of 1064 nm and a frequency of 5 Hz. Transmissivity of the chamber window was 76% at this laser-pulse wavelength. The laser pulse was focused by a lens of focal length 200 mm. The spot size of the laser pulse at the sample surface was about 1 – 1.5 mm in diameter. This pulse formed a luminescent plasma on the ice surface, and this luminescence was picked up by a single-core optical fiber. The luminescence spectrum was recorded by a multichannel photodetector (Princeton model SMA). The spectra were analyzed using the data-processing program of Ito *et al.* (1995) and Nakamura *et al.* (1996).

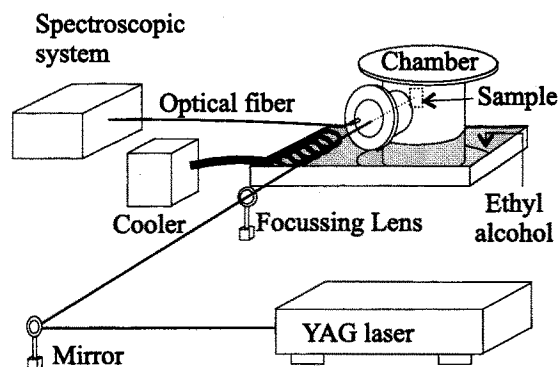


Fig. 2. Schematic of the experimental setup.

4. Results and discussion

Figure 3 shows an emission spectrum from a laser-induced plasma at the surface of ice containing $1000 \mu\text{g g}^{-1}$ of Na. This spectrum is the accumulation of 100 pulses measured from 500 to 3500 ns after the laser pulses. The laser energy was $600 \text{ mJ pulse}^{-1}$. We identified the peaks near 568 and 589 nm. Although the 589 nm peak consists of the well known DI and DII lines of Na at 589.5924 nm and 588.9950 nm (Reader and Corliss, 1987), these two lines were not resolved by our detection system. We used the peak around 589 nm, the strongest emission line of Na (Reader and Corliss, 1987), to evaluate its emission intensity and S/N ratio for optimization of the experimental conditions. The observed volume of sample used to measure

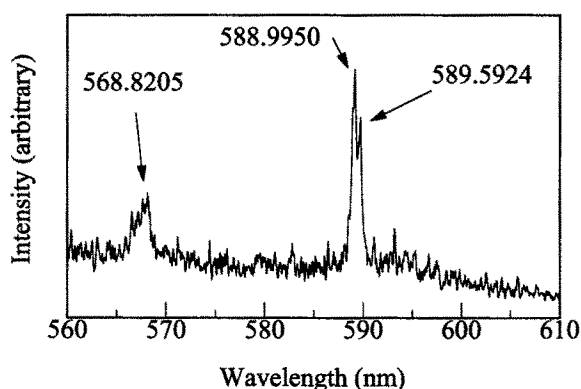


Fig. 3. Luminescence spectrum obtained for an ice sample with $1000 \mu\text{g g}^{-1}$ Na.

the spectrum was only about 1 mm across and 1 mm deep. Laser pulses of our laser system were invisible because the wavelength was in the infrared radiation range. But there is widespread use of improved laser systems that mix visible and infrared laser pulses so that the laser irradiation point at the sample becomes visible. With the use of such an improved laser system, we should be able to increase the positioning accuracy and spatial resolution to 1 – 2 mm.

A laser-induced plasma changes very quickly after laser pulse irradiation; the plasma expands out into the surrounding gas, thus forming a shock wave, and its temperature varies with time and position (e.g. Radziemski *et al.*, 1983; Cremers, *et al.*, 1984). Therefore, the luminescence signal from a plasma also changes with time, and thus the optimal timing of the spectral measurement needs to be determined. Optimal conditions of delay time and gate width for ice samples containing Na were determined so as to obtain high S/N spectra, as were done for ice samples containing Ca (Takata *et al.*, 2000). Here, delay time means the interval between the laser pulse and start of the spectral measurement, and the gate width means the spectrum measuring time.

First, we varied the delay time from 100 to 1800 ns with a fixed gate width of 2000 ns using ice samples containing $1000 \mu\text{g g}^{-1}$ Na. The laser was operated at $300 \text{ mJ pulse}^{-1}$ and the data were accumulated for 200 laser pulses. Figure 4a shows the resulting S/N ratio as a function of the delay time. The optimal delay time having the largest S/N was 600 – 1200 ns. Then, we varied the gate width from 800 to 3500 ns with the fixed optimal delay time of 1200 ns using ice samples containing $100 \mu\text{g g}^{-1}$ of Na (Fig. 4b). The laser operation and the data accumulation number were same with the experiment of the delay time varied. The optimal gate width was 2000 – 3000 ns.

The laser-induced plasma and the emission from the plasma fluctuated because the laser pulse intensity fluctuated significantly and laser-induced breakdown is highly nonlinear. However, the spectrum quality

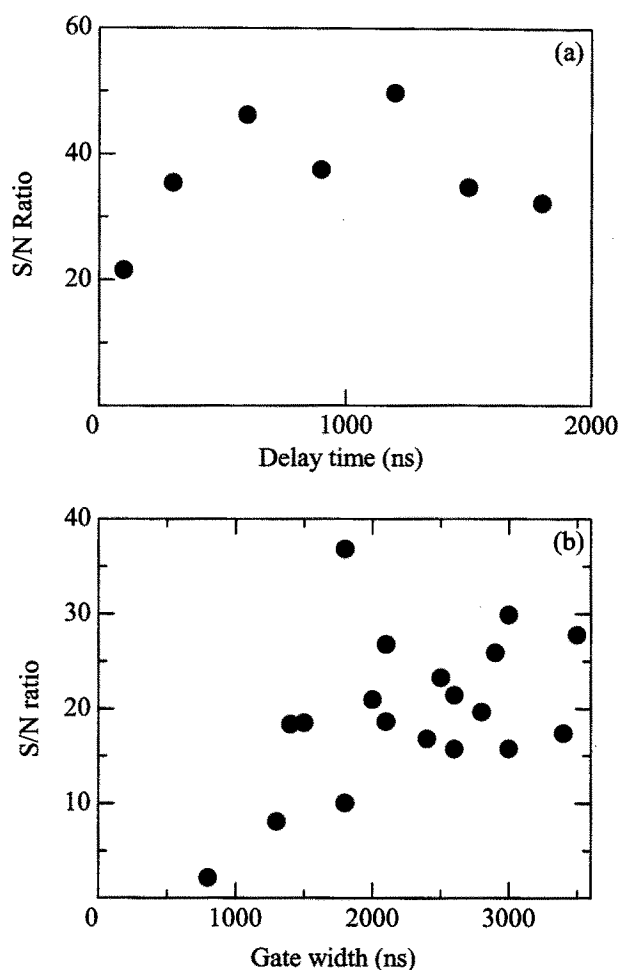


Fig. 4. Temporal change of S/N ratio around 589 nm for ice containing Na. (a) Dependence on delay time. (b) Dependence on gate width.

should become more stable as the number of accumulated laser pulses increases. In addition, fluctuations in the background emission, which contributes to noise, occur randomly and will be smoothed out with increasing number of accumulated laser pulses, whereas the real signal accumulates and adds up. Hence, the larger the number of pulses, the better the S/N ratio and the lower the detection limit. On the other hand, because the laser breakdown at the surface of ice causes some ice ablation, too many pulses would consume the ice near the focal point, which would decrease the emission intensity. Therefore, the number of laser pulses that maximizes S/N should be found. In the previous study (Takata *et al.*, 2000), we obtained the optimal pulse number of 250 – 300 for a low energy fluence EF of $13 \text{ J cm}^{-2} \text{ pulse}^{-1}$, which was just enough to generate a plasma (Takata *et al.*, 2000). In this study, the laser was operated at $600 \text{ mJ pulse}^{-1}$ and the irradiated area at the sample surface was about 1.5 mm across; therefore, the EF was about $26 \text{ J cm}^{-2} \text{ pulse}^{-1}$. When the EF was larger, the samples sometimes cracked after a few pulses. Figure 5 shows the S/N ratio versus the number of accumulated laser pulses. The experiment was done using samples

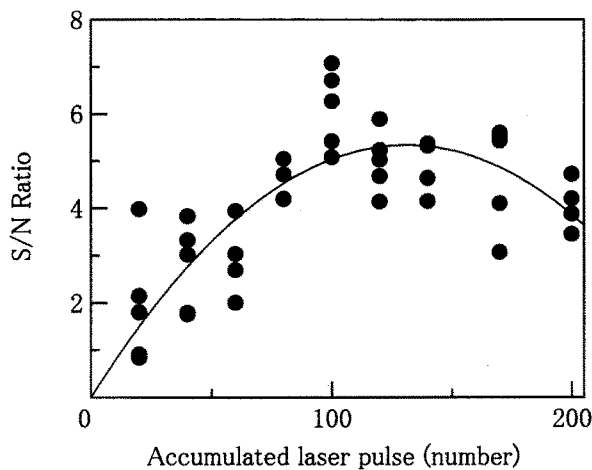


Fig. 5. Dependence of S/N ratio on the number of laser pulses. Laser power was $600 \text{ mJ pulse}^{-1}$ and the irradiated spot on the ice sample was 1.5 mm in diameter. The curve represents the result of secondary parabolic approximation by the least mean square method based on individual data.

containing $50 \mu\text{g g}^{-1}$ Na with the optimal delay time of 1000 ns and optimal gate width of 2500 ns . The S/N ratio increases with the accumulation of laser pulse up to 140 pulses and decreases with additional pulses. The optimal number of accumulated laser pulses is 140 under this laser operation.

We now discuss the optimal number of laser pulse accumulation by comparing our results for two energy fluences. The total integrated energy per unit area was $32 - 39 \text{ J mm}^{-2}$ for an EF of $13 \text{ J cm}^{-2} \text{ pulse}^{-1}$ and was 36 J mm^{-2} for an EF of $26 \text{ J cm}^{-2} \text{ pulse}^{-1}$. These values are close to each other, which suggests that the optimal number of laser pulses can be estimated so as to give the optimal total integrated energy per unit area of $30 - 40 \text{ J mm}^{-2}$.

The relation between Na concentration and emission intensity was examined using ice samples with the following Na concentrations: $1 \mu\text{g g}^{-1}$, $10 \mu\text{g g}^{-1}$, $25 \mu\text{g g}^{-1}$, $50 \mu\text{g g}^{-1}$, $100 \mu\text{g g}^{-1}$, $150 \mu\text{g g}^{-1}$, and $200 \mu\text{g g}^{-1}$. Experiments were done under the optimal conditions discussed above: the laser was operated at $300 \text{ mJ pulse}^{-1}$, the irradiation area was about 1.5 mm across, the delay time was 1200 ns , the gate width was 2500 ns , and data were accumulated for 200 laser pulses. The number of laser pulses was close to the optimal number because the total integrated energy per unit area was 26 J mm^{-2} , which was close to the optimal value of $30 - 40 \text{ J mm}^{-2}$.

Figure 6 shows the emission intensity (peak area) of Na ions around 589 nm versus Na concentration. We measured more than 7 samples for each concentration. Filled dots are data for individual samples and open dots are averages at a fixed concentration. The correlation is linear, and the correlation coefficient between the averaged peak areas and concentration is

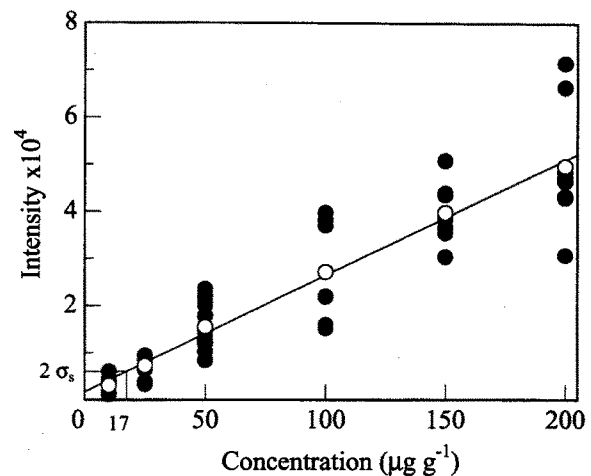


Fig. 6. Correlation between peak intensity around 589 nm and Na concentration for the concentration range of $1 - 200 \mu\text{g g}^{-1}$. Filled dots represent results on single samples and open dots represent averages over all samples with the same concentrations. The straight line represents the result of linear fitting by the least mean square method based on the average data. Seven or eight samples were measured for 10, 25, 100, 150 and $200 \mu\text{g g}^{-1}$, and fifteen samples were measured for $50 \mu\text{g g}^{-1}$.

0.99. Na emission around 589 nm was detected for all samples with Na concentrations larger than $10 \mu\text{g g}^{-1}$, but it was not detected for samples with Na concentration of $1 \mu\text{g g}^{-1}$. To evaluate the detection limit, we calculated the standard deviation σ of the emission intensities (peak area) at 10 and $25 \mu\text{g g}^{-1}$ with respect to the fitted line. The detection limit is approximately $17 \mu\text{g g}^{-1}$ based on the value of 2σ . Although a high correlation coefficient between the average emission intensity and concentration was obtained, at a given concentration, there was significant scatter in the intensities from different samples. The scatter can be due to a nonuniform distribution of ions in ice samples, unevenness of ice density in the irradiated area, or inherent fluctuations of emission intensity (Takata *et al.*, 2000). The major source of scatter in these experiments was most likely a nonuniform distribution of ions in the ice samples, and to a lesser degree, fluctuations in sample density. This is because the local sample density can vary even though the bulk density does not vary significantly. We checked the relation between the measured emission intensity and sample density for a fixed Na concentration; qualitatively, the intensity decreased as density decreased. In spite of the significant scatter in the data, our results suggest that several measurements average out the inhomogeneous distribution of ions and the fluctuation of sample density, and thus we can obtain a reasonable regression curve using average values of several samples.

Figure 6 indicates that we can determine Na in the range of $10 - 200 \mu\text{g g}^{-1}$ in ice samples by LIBS. We also investigated the use of LIBS on ice samples

with higher concentrations ($10 - 1000 \mu\text{g g}^{-1}$). The results also showed linear relation between the emission intensity and Na concentration for the range of $10 - 1000 \mu\text{g g}^{-1}$ ($r = 0.99$) as shown in Fig. 7. This suggests that we can apply the LIBS technique to sea ice samples, which contain high Na concentrations. However, we must measure the $0.1 - 1 \mu\text{g g}^{-1}$ concentration range for determination of Na in ice cores from coastal regions (e.g. Mulvaney and Wolff, 1994; Watanabe *et al.*, 2001), and polar inland ice cores contain $10 - 10^2$ times less Na than those in coastal regions.

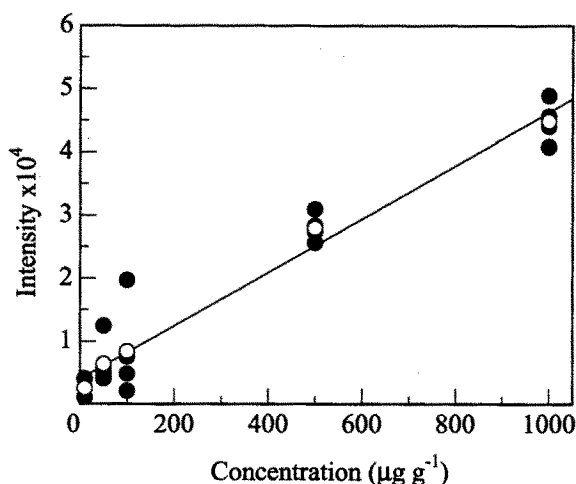


Fig. 7. Correlation between peak intensity around 589 nm and Na concentration for the concentration range of $10 - 1000 \mu\text{g g}^{-1}$. Notation of filled dots, open dots and the straight line are the same as that in Fig. 6.

To analyze ice core samples, a more sensitive detection method than the simple time-resolved emission spectrometry employed here should be developed for ice samples. Possible methods include the double LIBS method (Nakamura *et al.*, 1996), laser induced fluorometry technique, and mass spectroscopy.

5. Conclusions

We developed a new method to prepare artificial ice samples containing given concentrations of Na, and applied the LIBS technique to determine Na concentrations in solid ice samples. The optimum conditions for laser irradiation and timing of spectral measurement to obtain a high S/N ratio and low detection limit were examined. The optimum delay time and gate width were $600 - 1200 \text{ ns}$ and $2000 - 3000 \text{ ns}$, respectively. The optimal total integrated energy per unit area was estimated to be $30 - 40 \text{ J mm}^{-2}$. We found a linear relationship between Na concentration and mean emission intensity in the concentration ranges from 10 to $200 \mu\text{g g}^{-1}$ and 10 to $1000 \mu\text{g g}^{-1}$. The detection limit was $17 \mu\text{g g}^{-1}$. Thus, our results indicate that LIBS can be used to determine Na

concentrations in sea ice. Although the current detection limit is presently too high to analyze ice core samples, LIBS has great potential as a non-destructive technique with very high sampling resolution of the order of mm because the sample volume that was consumed was only 1 mm in both diameter and depth. As a future study, we plan to develop a method to prepare more homogenous standard ice samples that will reduce the data scatter. We also need to decrease the detection limit to analyze ice core samples.

Acknowledgments

We thank Prof. T. Umemura and Dr. S. Kamimura for their helpful comments on the investigations, and Dr. S. Nakamura and Mr. N. Sasaki for their support to our experiments. We also thank the staff at Nagaoka Institute of Snow and Ice Studies for their help with sample preparation.

References

- Cremers, D. A. and Radziemski, L. J. (1983): Detection of chlorine and fluorine in air by laser-induced breakdown spectrometry. *Anal. Chem.*, **55**, 1252-1256.
- Cremers, D. A., Radziemski, L. J. and Loree, T. R. (1984): Spectrochemical analysis of liquids using the laser spark. *Appl. Spectrosc.*, **38**(5), 721-729.
- Iida, Y. (1990): Effects of atmosphere on laser vaporization and excitation processes of solid samples. *Spectrochim. Acta*, **45B**(12), 1353-1367.
- Ito, Y., Ueki, O. and Nakamura, S. (1995): Determination of colloidal iron in water by laser-induced breakdown spectroscopy. *Anal. Chim. Acta*, **299**, 401-405.
- Kagawa, K. and Yokoi, S. (1982): Application of the N^2 laser microprobe spectrochemical analysis. *Spectrochim. Acta*, **37B**(9), 789-795.
- Kagawa, K., Hattori, H., Ishikane, M., Ueda, M. and Kurniawan, H. (1995): Atomic emission spectrometric analysis of steel and glass using a TEA CO_2 laser-induced shock wave plasma. *Anal. Chim. Acta*, **299**, 393-399.
- Kitamori, T., Matsui, T., Sakagami, M. and Sawada, T. (1989): Laser breakdown spectrochemical analysis of microparticles in liquids. *Chem. Lett.*, 2205-2208.
- Meese, D. A., Gow, A. J., Alley, R. B. Zielinski, G. A., Grootes, P. M., Ram, M., Tayler, K. C. Mayewski, P. A. and Bolzan, J. F. (1997): The Greenland Ice Sheet Project 2 depth-age scale: Method and results. *J. Geophys. Res.*, **102**(C12), 26411-26423.
- Mulvaney, R. and Wolff, E. W. (1994): Spatial variability of the major chemistry of the Antarctic ice sheet. *Ann. Glaciol.*, **20**, 440-447.
- Nakamura, S., Ito, Y., Sone, K., Hiraga, H. and Kaneko, K. (1996): Determination of an iron suspension in water by laser-induced breakdown spectroscopy with two sequential laser pulses. *Anal. Chem.*, **68**, 2981-2986.
- Oeschger, H. and Langway, C. C. Jr. eds. (1989): *The environmental record in glaciers and ice sheets*. John Wiley and sons, New York, 400pp.
- Radziemski, L. J., Loree, T. R., Cremers, D. A. and Hoffman, N. M. (1983): Time-resolved laser-induced breakdown spectrometry of aerosols. *Anal. Chem.*, **55**, 1246-1252.
- Radziemski, L. J., and Cremers, D. A. (1989): Spectrochemical

- analysis using laser plasma excitation., eds. Radziemski, L. J. and Cremers, D. A. Laser-induced plasmas and applications, Merce Dekker Inc., New York, 295-325.
- Reader, J. and Corliss, C. H. eds. (1987): Line Spectra of the elements. ed. Weast, R. C., 67th edition, CRC handbook of chemistry and physics, CRC Press, Boca Raton, E201-E327.
- Reid, A. P., Potts, W. T. W., Oates, K., Mulvaney, R. and Wolff, E. W. (1992): Preparation of aqueous standards for low temperature X-ray microanalysis. *Microsc. Res. Tec.*, **22**, 207-211.
- Röthlisberger, R., Bigler, M., Hutterli, M., Sommer, S. and Stauffer, B. (2000): Technique for continuous high-resolution analysis of trace substances in firn and ice cores. *Environ. Sci. Technol.*, **34**(2), 338-342.
- Sigg, A., Fuhrer, K., Anklin, M., Staffelbach, T. and Zurmühle, D. (1994): A continuous analysis technique for trace species in ice cores. *Environ. Sci. Technol.*, **28**(2), 204-209.
- Takata, M., Ito, Y., Goto-Azuma, K. and Azuma, N. (2000): An attempt at determination of calcium in ice by laser induced breakdown spectroscopy. *Bull. Glacier Res.*, **17**, 37-42.
- Watanabe, O., Motoyama, H., Igarashi, M., Kamiyama, K., Matoba, S., Goto-Azuma, K., Narita, H. and Kameda, T. (2001): Studies on climatic and environmental changes during the last few hundred years using ice cores from various sites in Nordaustlandet, Svalbard. *Mem. Natl Inst. Polar Res., Spec. Issue* **54**, 227-242.
- Weeks, W. F. and Ackley, S. F. (1982): The growth, structure, and properties of sea ice. *CRREL Monograph*, **82**(1), 136pp.
- Wyness, L. E., Morris, J. A. Oates, K., Staff, W. G. and Huddart, H. (1987): Quantative X-ray microanalysis of bulk hydrated specimens: A method using gelatine standards. *J. Pathol.*, **153**, 61-69.